Atmospheric Environment 43 (2009) 604–618

Contents lists available at ScienceDirect

Atmospheric Environment

journal homepage: www.elsevier.com/locate/atmosenv

The global impact of ozone on agricultural crop yields under current and future air quality legislation

Rita Van Dingenen [a,*], Frank J. Dentener [a], Frank Raes [a], Maarten C. Krol [b], Lisa Emberson [c], Janusz Cofala [d]

[a] European Commission – DG Joint Research Centre, Institute for Environment and Sustainability, Ispra, Italy
[b] Department of Meteorology and Air Quality, Wageningen University and Research Centre (WUR), Wageningen, The Netherlands
[c] Stockholm Environment Institute, University of York, Biology Dept., York, UK
[d] International Institute for Applied Systems Analysis, Laxenburg, Austria

ARTICLE INFO

Article history:
Received 11 March 2008
Received in revised form
19 July 2008
Accepted 2 October 2008

Keywords:
Ozone
Crop damage
Global
Model
Impact assessment

ABSTRACT

In this paper we evaluate the global impact of surface ozone on four types of agricultural crop. The study is based on modelled global hourly ozone fields for the year 2000 and 2030, using the global $1^\circ \times 1^\circ$ 2-way nested atmospheric chemical transport model (TM5). Projections for the year 2030 are based on the relatively optimistic "current legislation (CLE) scenario", i.e. assuming that currently approved air quality legislation will be fully implemented by the year 2030, without a further development of new abatement policies. For both runs, the relative yield loss due to ozone damage is evaluated based on two different indices (accumulated concentration above a 40 ppbV threshold and seasonal mean daytime ozone concentration respectively) on a global, regional and national scale. The cumulative metric appears to be far less robust than the seasonal mean, while the seasonal mean shows satisfactory agreement with measurements in Europe, the US, China and Southern India and South-East Asia.

Present day global relative yield losses are estimated to range between 7% and 12% for wheat, between 6% and 16% for soybean, between 3% and 4% for rice, and between 3% and 5% for maize (range resulting from different metrics used). Taking into account possible biases in our assessment, introduced through the global application of "western" crop exposure–response functions, and through model performance in reproducing ozone-exposure metrics, our estimates may be considered as being conservative.

Under the 2030 CLE scenario, the global situation is expected to deteriorate mainly for wheat (additional 2–6% loss globally) and rice (additional 1–2% loss globally). India, for which no mitigation measures have been assumed by 2030, accounts for 50% of these global increase in crop yield loss. On a regional-scale, significant reductions in crop losses by CLE-2030 are only predicted in Europe (soybean) and China (wheat).

Translating these assumed yield losses into total global economic damage for the four crops considered, using world market prices for the year 2000, we estimate an economic loss in the range $14–$26 billion. About 40% of this damage is occurring in China and India. Considering the recent upward trends in food prices, the ozone-induced damage to crops is expected to offset a significant portion of the GDP growth rate, especially in countries with an economy based on agricultural production.

1. Introduction

Field experiments have demonstrated that atmospheric ozone can damage crops, leading to yield reduction and a deteriorating crop quality (Krupa et al., 1998). The resulting economic losses and threat to food security has become an issue of concern in world regions where the expanding economy has lead to an increased emission of air pollutants in general and ozone precursors in particular (Holland et al., 2002; Adams et al., 1982; Li et al., 1999; Wang and Mauzerall, 2004; Aunan et al., 2000).

In Europe and the US, air quality guidelines for ozone have been established in order to protect human health and vegetation. In Europe, the standard for the protection of vegetation against ozone damage is expressed as a critical level of accumulated ozone concentration above a threshold of 40 ppbV (AOT40) which should not be exceeded during the growing season (3 ppm h for agricultural crops, 5 ppm h for forests). In the US, the current secondary ozone standard designed to protect human welfare (which includes vegetation) has been proposed to be set equal to the standards to protect human health (the maximal 8 h average ozone concentration of 75 ppbV

* Corresponding author.
E-mail address: rita.van-dingenen@jrc.it (R. Van Dingenen).

1352-2310/$ – see front matter © 2008 Elsevier Ltd. All rights reserved.
doi:10.1016/j.atmosenv.2008.10.033

should not be exceeded more than 3 times per year, with the average fourth highest concentration over a 3-year period determining whether a location is out of compliance).

Attempts to adhere to these guidelines have led to a reduction in the occurrence of ozone peak levels since the 1990s (Solberg and Lindskog, 2005; Lin et al., 2001). Rapidly growing economies, in particular those in East, South-East Asia and South Asia, however, have experienced continued deterioration of their air quality due to increasing emissions of nitrogen oxides and other pollutants, and these trends are expected to continue as economies continue to expand.

Since the 1980s, extensive field studies in the US (National Crop Loss Assessment Network, NCLAN) and in Europe (European Open Top Chamber Programme, EOTCP) have attempted to establish crop-specific exposure–response functions which relate a quantifiable ozone-exposure indicator to a reduction in the crop yield (Heck et al., 1987; Legge et al., 1995; Fuhrer et al., 1997). Mauzerall and Wang (2001) give a comprehensive overview of the various indicators that have been developed and applied in Europe and the U.S. since the NCLAN and EOTCP studies. Most frequently used indicators are seasonal 7 h and 12 h mean ozone concentration during daylight (M7 and M12 respectively) and seasonal cumulative exposure over a threshold such as 60 ppbV and 40 pbbV (SUM06 and AOT40 respectively). Recently, Mills et al. (2007) re-compiled a large number of crop-response data from existing literature for 19 crops, many of which originally based on 7 h and 24 h means, in order to derive all response functions as a function of AOT40.

The availability of regional air pollution models with a high spatial and temporal resolution makes it possible to combine modelled ozone fields, exposure–response functions, crop location and growing season, to obtain global and regional estimates of crop losses. Aunan et al. (2000) evaluated losses of rice, wheat, soybeans and maize in China, for the base year 1990 as well as projected losses for 2020 based on the projected evolution of GDP and associated energy demand (pre-SRES scenario, van Aardenne et al., 1999). A similar study was performed by Wang and Mauzerall (2004) (hereafter W&M04) for China, Korea and Japan, using the IPCC B2 scenario for 2020. Both studies concluded that present day surface ozone already causes substantial crop losses in this region (in particular for sensitive crops like soybean and spring wheat) and that significant additional losses may be expected (in the order of 30% yield loss) by 2020 under the emission scenarios considered. At the same time these studies pointed out that the uncertainty on these loss estimates is large and that there is little consistency between exposure–response functions based on various ozone quality indices.

Holland et al. (2006) estimated crop losses and the associated economic loss in Europe for 23 horticultural and agricultural crops for the base year 2000, as well as a set of emission scenarios for 2020. Results for 2000 indicate an overall loss of 3% of all crop species considered (equivalent to €6.7 billion economic damage), reducing to 2% under an "implementation of current legislation" (CLE) scenario for 2020 (€4.5 billion damage).

All these and earlier local and regional studies indicate that a substantial economic benefit may be expected from a reduction in air pollution. However, due to a lack of consistency in the used methodology for calculating crop damage, as well as for the economic impact, the mentioned regional results are difficult to compare to each other. A globally consistent estimate of crop losses due to air pollution, in all relevant world regions, based on a consistent emission inventory and modelling approach, has not been performed to our knowledge.

In this study, we apply the global chemical transport model TM5, taking advantage of its feature to provide regional zooms with a $1^\circ \times 1^\circ$ horizontal resolution within a global domain. The model was developed for global studies which require high resolution regionally while a coarser resolution over region of low relevance is acceptable (Krol et al., 2005). We explore the impact of implementing current Air Quality Legislation (CLE), comparing model runs for the base case (year 2000) with the CLE emission scenario for the year 2030, assuming that all currently decided policies have been fully implemented. Using this rather optimistic scenario we evaluate the potential that existing legislation has to mitigate elevated O_3 concentrations and associated crop losses. The model runs were obtained in the frame of the ACCENT-PHOTOCOMP-2030 multi-model exercise (Dentener et al., 2006; Stevenson et al., 2006) (ACCENT: Atmospheric Composition Change: the European NeTwork of excellence).

2. Methodology

We will evaluate the global risk of crop damage due to ozone, for 4 major crops (wheat, rice, maize and soybeans), based on 2 different exposure indicators: (1) the seasonal mean daytime ozone concentration (indicated as M7 for the 7 h mean (09:00–15:59) and M12 for the 12 h mean (08:00–17:59)), and (2) the accumulated daytime hourly ozone concentration above a threshold of 40 ppbV (AOT40). The choice of M7/M12 and AOT40 is guided by the fact that exposure–response functions are available from literature for all four crops considered, and that our results can be compared with those of earlier studies mentioned before. Further, AOT40 has been favoured in Europe as the concentration-based indicator for ozone effects on crops (Fuhrer et al., 1997). Note that we consider M7 and M12 as one indicator type. Over land, M12 is in general only slightly lower than M7 and both parameters are obviously highly correlated. The only reason for considering both is that the available exposure–response (E–R) functions for wheat and rice are expressed as a function of M7 whereas those for maize and soybean are expressed as a function of M12.

The definition of the indicators and their corresponding E–R function, which expresses the crop relative yield (RY) as a function of the respective indicator for each of the crops, is given in Table 1. The E–R functions based on M7 and M12 are taken from W&M04, and have a Weibull functional form. Those expressed as a function of AOT40 are obtained from Mills et al. (2007) and are linear. It is

Table 1
Overview of air quality indices used to evaluate crop yield losses. The *a* and *b* coefficients refer to the exposure–reponse equations in Table 2. All O_3 concentrations refer to hourly values.

References	Index	Unit	Definition	Exposure/dose–response function: relative yield loss (RYL)	Wheat		Rice		Soy		Maize	
					a	*b*	*a*	*b*	*a*	*b*	*a*	*b*
Wang and Mauzerall, 2004	M7	ppbV	7-Hour seasonal O_3 mean 3 months, 9:00–15:59	$1-\exp[-(M7/a)^b]/\exp[-(25/a)^b]$	137	2.34	202	2.47				
Wang and Mauzerall, 2004	M12	ppbV	12-Hour seasonal O_3 mean 3 months, 8:00–19:59	$1-\exp[-(M12/a)^b]/\exp[-(20/a)^b]$					107	1.58	124	2.83
Mills et al., 2007, corrected for offset (see text)	AOT40	ppm h	$\sum_{i=1}^{n}[O_3]_i - 40, [O_3] \geq 40$ ppbV 3 months, 8:00–19:59	*a*AOT40	0.0163		0.00415		0.0113		0.00356	

important to realize that these E–R relationships are 'pooled' from a variety of cultivars grown in the US and Europe. They are considered to reliably represent the average response of the commonly grown cultivar population on national or regional level in those regions, without having the need to deal with individual cultivar distribution (Adams et al., 1987). Because of lacking experimental E–R data for Asia and Africa, we have applied the same functions globally. Small scale individual studies indicate that Asian cultivars for winter wheat and rice are equally or more sensitive to ozone damage than the US cultivars (Aunan et al., 2000), hence applying the US-derived E–R relationship leads to a conservative result. Apart from genotype-related differences in sensitivity, the crop-response will also depend on ambient conditions like temperature, humidity, soil type, …, factors which have not been considered in the currently applied E–R relationships. In fact, the LRTAP (Long-Range Transboundary Air Pollution) convention now recognises the importance of deriving an approach based on the actual flux of ozone through the plant stomata, taking into account all relevant environmental factors (see LRTAP Convention, 2004). As such, the enhanced risk of crops in warm and humid conditions (opened stomata) compared to dry conditions (closed stomata) is explicitly accounted for. At present, experimental data for deriving the ozone stomatal flux are only available for wheat and potato, hence we did not include this approach in the present study.

Two further issues have to be considered regarding the applied E–R functions.

(1) The AOT40-based E–R functions from Mills et al. (2007) have an intercept which is in general different from 1 (0.99, 0.94, 1.02, 1.02 for wheat, rice, maize and soybean respectively). In particular for rice, this causes an offset of 6% which is very high compared to the slope of the AOT40–RY relationship. Therefore, we scaled the E–R functions given by Mills et al. (2007) to their value at AOT40 = 0, such that the intercept of the relative yield equals 1.
(2) An intercomparison of the E–R functions for various indicators reveals an inherent inconsistency. This is illustrated in Fig. 1 where the relative yield loss (RYL = 1 − RY) from AOT40 is plotted against the RYL obtained from M7 or M12 for 4 different crops. The indicator values are calculated from measured hourly ozone data for 178 quality-controlled measurement stations, pertaining to established monitoring networks in and outside Europe (EMEP, AirBase, WMO). For wheat and rice, M7 results in significantly lower losses than a loss calculation based on AOT40 (74% and 64% lower respectively). For maize and soybeans, M12 losses are higher than those based on AOT40, but the deviation from the 1:1 line is smaller than for the former crops (24% and 28% higher respectively). These differences in calculated RYL from cumulative and mean metrics have been noted before (Aunan et al., 2000; W&M04). They may be a result of the statistical methods used to derive the E–R functions in the respective studies, or may reflect differences in plant sensitivities to differing O_3 distributions and to high O_3 concentrations. In particular for wheat, this leads to a large range in estimated yield loss from both indicators.

2.1. General approach of the global evaluation of crop losses

We follow the approach outlined by W&M04 and Holland et al., 2006. Fig. 2 shows the steps involved in the analysis. Starting from the global $1^\circ \times 1^\circ$ modelled hourly ozone fields, the respective indicators are averaged (M7/M12) or accumulated (AOT40) over the appropriate growing season, leading to a gridded ($1^\circ \times 1^\circ$) relative yield loss (RYL) calculation for each relevant crop. The RYL field is overlaid with the $1^\circ \times 1^\circ$ crop production grid which has been derived from national or regional production numbers. The methodology for obtaining crop spatial distribution and start of the growing season on a $1^\circ \times 1^\circ$ resolution is described in more detail below. For each grid cell, the crop production loss (CPL_i) is calculated from the RYL and the actual crop production for the year 2000 within the grid cell (CP_i):

$$CPL_i = \frac{RYL_i}{1 - RYL_i} \times CP_i$$

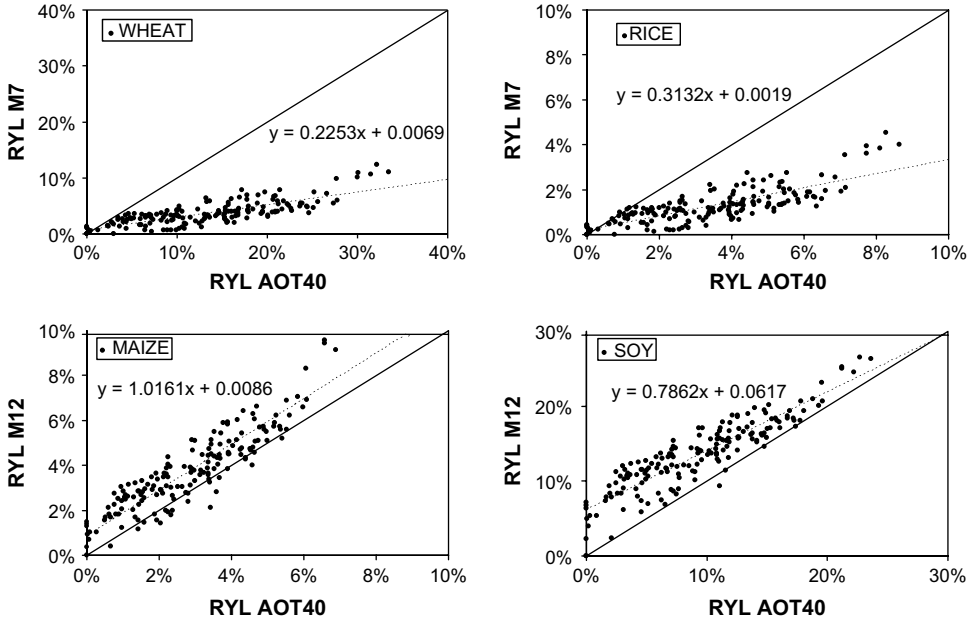

Fig. 1. Relative yield loss based on 3-monthly M7 (wheat, rice) or M12 (maize, soybeans) as indicator vs. relative yield loss based on AOT40. Indicator values are derived from hourly measurements. Each point represents a single measurement station from EMEP, Airbase and WMO-GAW measurement network.

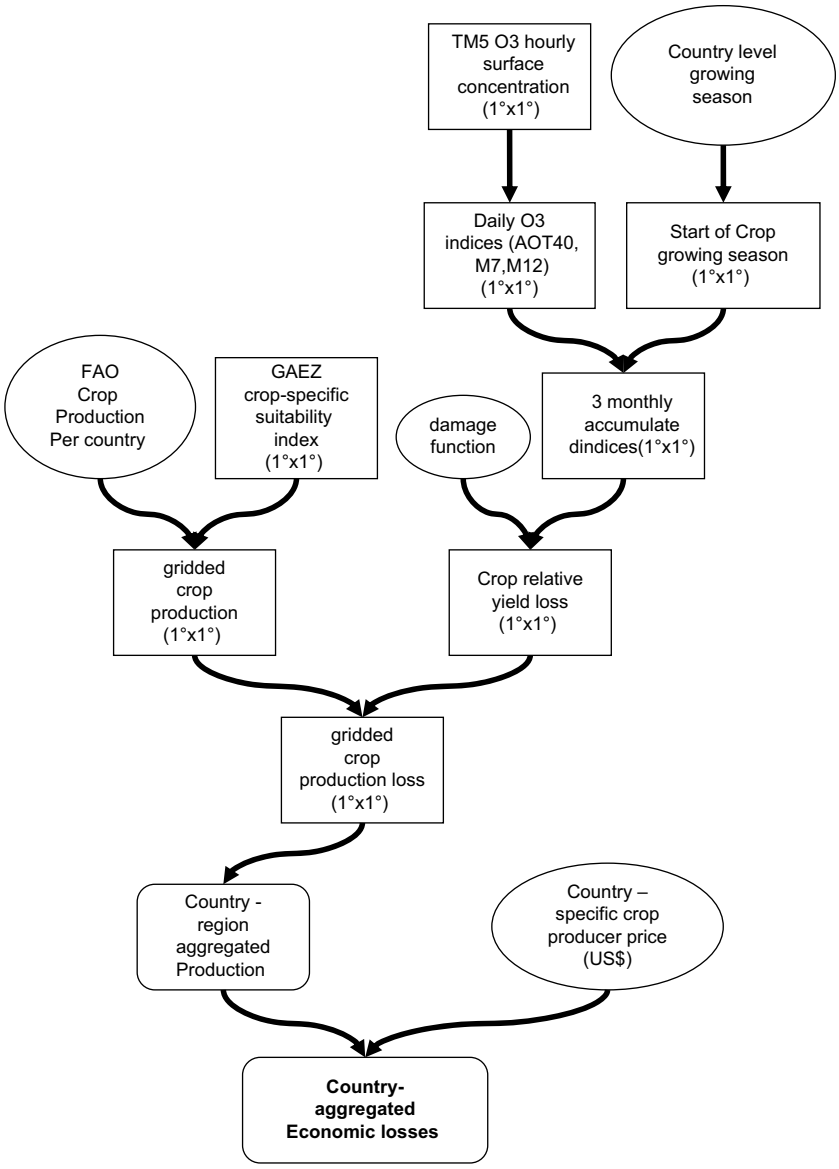

Fig. 2. General outline of the different steps involved in the data analysis.

The national CPL is then obtained by summing up all grid cells belonging to each country. The economic damage is estimated by multiplying CPL with the producer prices for the year 2000 (PP_{2000}) as given by FAOSTAT (http://faostat.fao.org, accessed December 2007). The producer prices are used as a proxy for the domestic market price, due to the lack of information on actual crop market prices.

$$EL = CPL \times PP_{2000}$$

PP_{2000} are not always available for some minor producing countries. In that case, we applied the median crop price for the year 2000, i.e. \$148/metric ton for wheat, \$138/metric ton for maize, \$202/metric ton for rice and \$205/metric ton for soybeans. The fraction of the global production for which no individual producer price is available is limited to 2.1% for wheat and maize, 6.3% for rice and 0.43% for soybeans.

By applying this simple cost calculation, we neglect possible feedbacks of changes in supply and the demand on the price evolution. Adams et al. (1982) estimated that the simple multiplication approach overestimates the damage by 20% by not accounting for economic adjustments and compensating price effects.

2.2. Crop distribution maps

Crop production numbers are generally available on national level. For a number of large countries, data are available at a higher resolution. For instance, The US Department of Agriculture (USDA) provides US production data for all crops on county level (http://www.usda.gov/nass/graphics/county00/indexdata.htm). For our analysis, we aggregated these high resolution US data to crop production at state level. For China, India, Canada and Brazil, the national production numbers for the relevant crops were distributed over provinces or states according to information provided by USDA, 1994.

The national or regional crop production (CP) was then distributed over the $1^\circ \times 1^\circ$ grids of each country (or state/province). The fraction of the total production attributed to each grid cell (CP_i) is based on the crop-specific Global Agro-Ecological Zones (GAEZ) suitability index, developed by Fischer et al. (2000). The crop suitability index (SI) is a modelled index, based on local soil and terrain properties, rainfall, temperature limitations, land use, … By lack of global gridded crop distribution maps based on

observations, the GAEZ suitability maps are probably the best ones available to describe the spatial distribution of individual crops. The production (metric tons) of crop k within grid cell i is given by:

$$CP_{i,k} = \frac{SI_{i,k} \times CP_k}{\sum_j SI_{j,k}}$$

$\sum_j SI_{j,k}$ is the sum of the suitability indices for crop k overall grid cells of the country, and consequently $\sum_j CP_{j,k} = CP_k$, the total production of the country.

Fig. 3 shows the resulting year 2000 global crop production maps for the wheat and rice. The maps for the other crops are available as Supplementary material.

2.3. Crop growing season

The definition of the ozone-exposure indicators requires averaging or accumulation of ozone concentration over a period of 3 months, starting at the beginning of the growing season.

The growing season for wheat was calculated using a phenological model, as recommended and described in the "Mapping Manual 2004" by LRTAP Convention, 2004. The model makes use of the available daily mean temperature, from which the time of mid-anthesis is calculated. Following the mapping manual, this happens when a temperature sum of 1075 °C days after the first frost-free day of winter is reached, taking into account a six month shift between temperate NH and SH. The

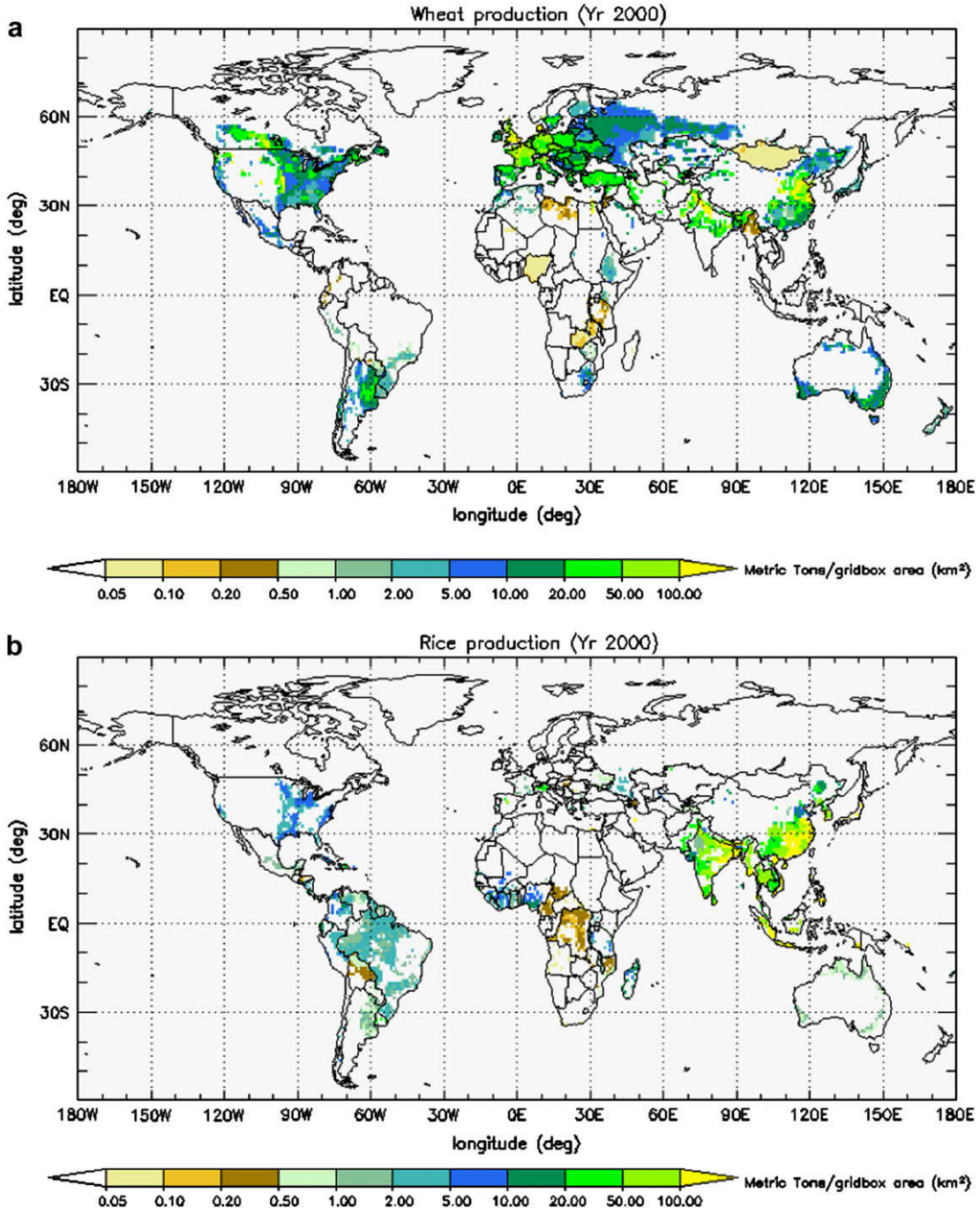

Fig. 3. Crop production maps for (a) wheat and (b) rice, calculated from national and regional production numbers and Agro-Ecological Zones suitability indices (see text).

start of the ozone-sensitive period (A_{start}) is situated 270 °C days before mid-anthesis, and the end of the period (A_{end}) 970 °C days after A_{start}. In order to have an identical accumulation period length for all regions, we define the wheat growing season as the 3-month (92 days) period preceding A_{end}. Using this approach we obtain a growing season defined at the resolution of 1 grid cell. The modelled growing season was cross-checked against national wheat growing season tables provided by USDA and LRTAP, 2004, and appears to be performing very well both in NH and SH.

For the other 3 crops we have no phenological model available. For maize and soybean, we made use of crop calendar tables published by USDA (1994), covering the major crop areas of the world. In our study, the growing season was defined as 3 months preceding the start of the harvest period. For countries identified as producers by FOA, but not listed in the USDA compilation, we apply the growing season from known countries in the same thermal climate zone within the (sub)continent. The thermal climate zones are taken from Fischer et al., 2000.

For rice, we allow up to 3 growing seasons. The periods and the fraction of total annual rice production within each period are compiled from USDA (1994), from tables published by the International Rice Research Institute (IRRI, http://www.irri.org/science/ricestat/accessed December 2006), and from W&M04.

Global maps of onset of the growing season for each crop are available as Supplementary material.

Although the timing of the growing season may be an important factor in the exposure to ozone and associated crop damage at the level of individual grid boxes or even small countries, regionally aggregated crop losses appear not to be very sensitive to the onset of the growing season. A recalculation of crop losses by shifting the growing season one month forward or backward, leads to a change in the calculated economic loss within 5% for Europe, and less than 2% for all other regions (including the globally aggregated loss).

3. Model and emission scenario

Global ozone for the year 2000 is calculated with the global chemistry transport model TM5 (Krol et al., 2005). The model is used for global studies which require high resolution regionally ($1° \times 1°$) but can work on a coarser resolution globally ($6° \times 4°$). The zoom algorithm introduces refinement in both space and time in some predefined regions, in this case Europe, North America and Asia. For this study no high resolution zoom over Africa and South America is available. Ozone levels over these regions are dominated by biomass burning, for which emission inventories are highly uncertain. Although the model is capturing well the timing of the biomass burning ozone episodes, a quantitative evaluation is difficult due to a lack of measurement data. Adding to this the uncertainties on crop distribution and growing season in this region, we focus our evaluation of regional losses and economic damage on the NH regions which account for most of the agricultural production.

The TM5 model operates with off-line meteorology from the European Centre for Medium range Weather Forecasts (ECMWF; 6 h IFS forecast), which is stored at a 6-hourly resolution for the large scale 3D fields, and 3-hourly for the parameters describing exchange processes at the surface. Of the 60 vertical layers in the ECMWF model, a subset of 25 layers is used within TM5, of which 5 layers represent the boundary layer, 10 the free troposphere, and the remaining 10 layers the stratosphere.

TM5 includes a coupled gas-phase chemistry and bulk aerosol chemistry, with the exception of dust and sea salt which are size-resolved.

Emissions for the reference year 2000 and the future scenario 'Current Legislation' (CLE, year 2030) were based on recent inventories developed by the International Institute for Applied System Analysis (IIASA, available at http://www.iiasa.ac.at/rains/global_emiss/global_emiss.html). The CLE scenario was based on legislation in place at the year 2001 and assumes full implementation by 2030. We note here that e.g. recent emission legislation in India, like the mandatory introduction of compressed natural gas (CNG) as fuel for public transport vehicles in New Delhi, was not included in this study, leading to a possibly overly pessimistic emission scenario for India.

The global totals of present and future emissions were distributed spatially according to EDGAR3.2 (Olivier and Berdowski, 2001) as described in Dentener et al., 2005. Fig. 4 shows the total NO_x emissions for the major world regions for 2000 and 2030 under the CLE scenario.

The model delivers global hourly ozone concentrations from the midpoint of the first layer which is about 60 m high. Due to deposition processes to the surface, trace gases in general show a concentration gradient within the lowest model layer. The default crop height generally being 1 m (2 m for maize), we recalculated the ozone concentration at crop canopy height, following the approach of LRTAP Convention (2004) and Tuovinen et al. (2007). Also the concentration at 10 m was derived, in order to compare modelled ozone concentrations with measurements. A detailed description of the approach followed is available as Supplementary material.

4. Results

4.1. Present and future global ozone surface concentration

Fig. 5 shows TM5 3-monthly averaged ozone for the four seasons of the year 2000 (a–d) and the expected change by 2030 (e–h) under the CLE scenario. The timing and location of elevated ozone levels varies strongly between different regions: North America, Europe (in particular the Mediterranean area) and industrial areas in China experience the highest O_3 levels of the order 60 ppbV during the NH summer season (JJA) whereas subtropical regions of Central America and India show their maximum ozone concentrations (50–60 ppbV) during MAM. The decline of ozone over the Indian subcontinent during JJA is related to the occurrence of the south-west monsoon and associated rainfall. Also in Central America, the rainy season from June till October prevents the build up of high surface O_3 levels like it is the case during spring. Over the African

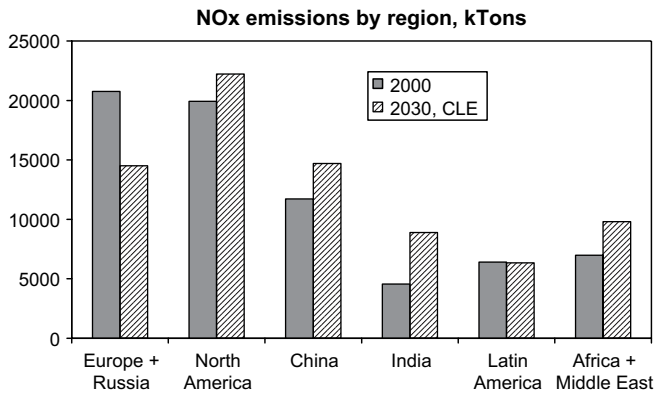

Fig. 4. Total NO_x emissions in the year 2000 and 2030 (CLE scenario) for major world regions.

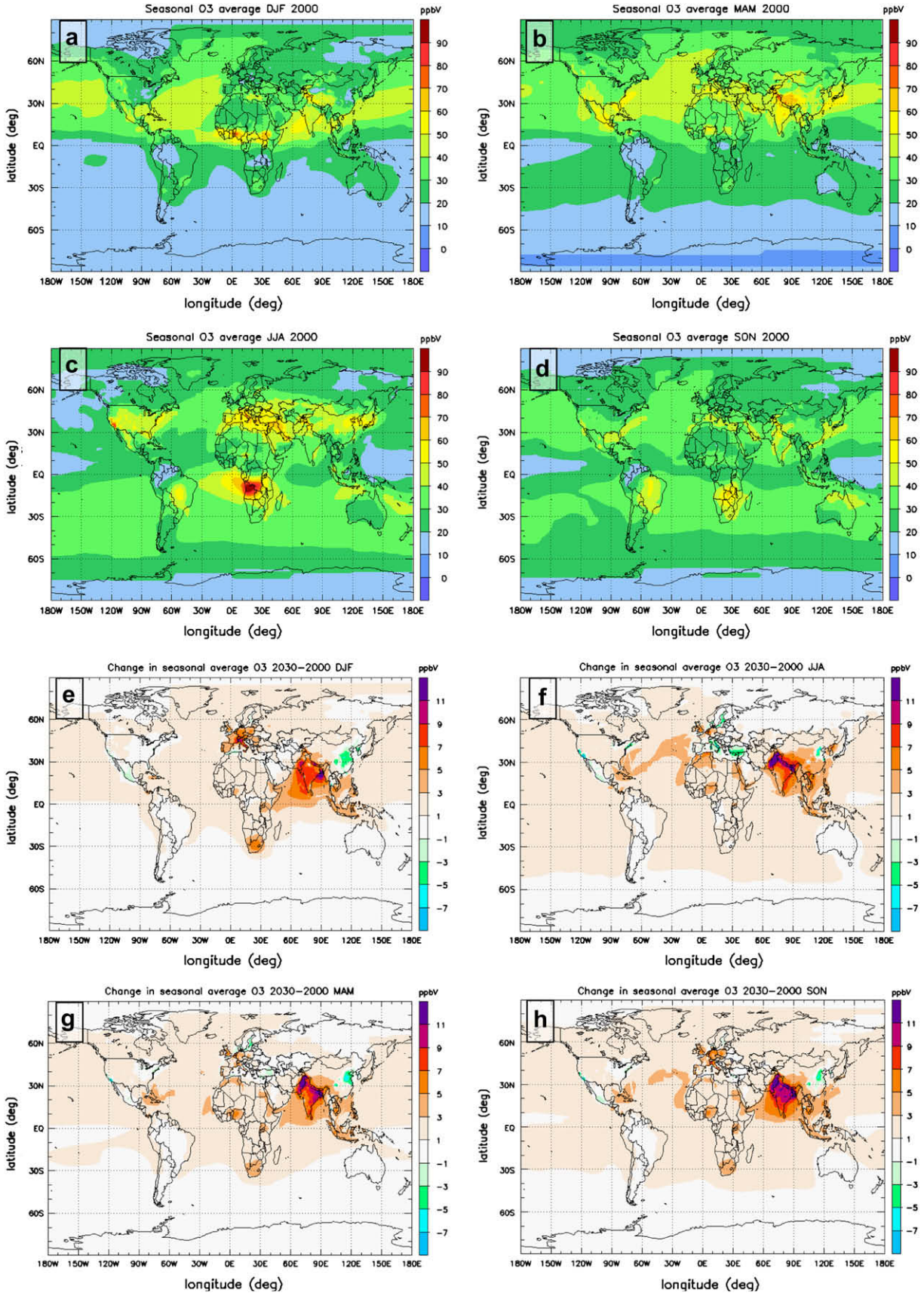

Fig. 5. (a–d) Seasonal average surface ozone for the year 2000 and (e–h) the change in seasonal surface ozone concentration by 2030 under a CLE scenario.

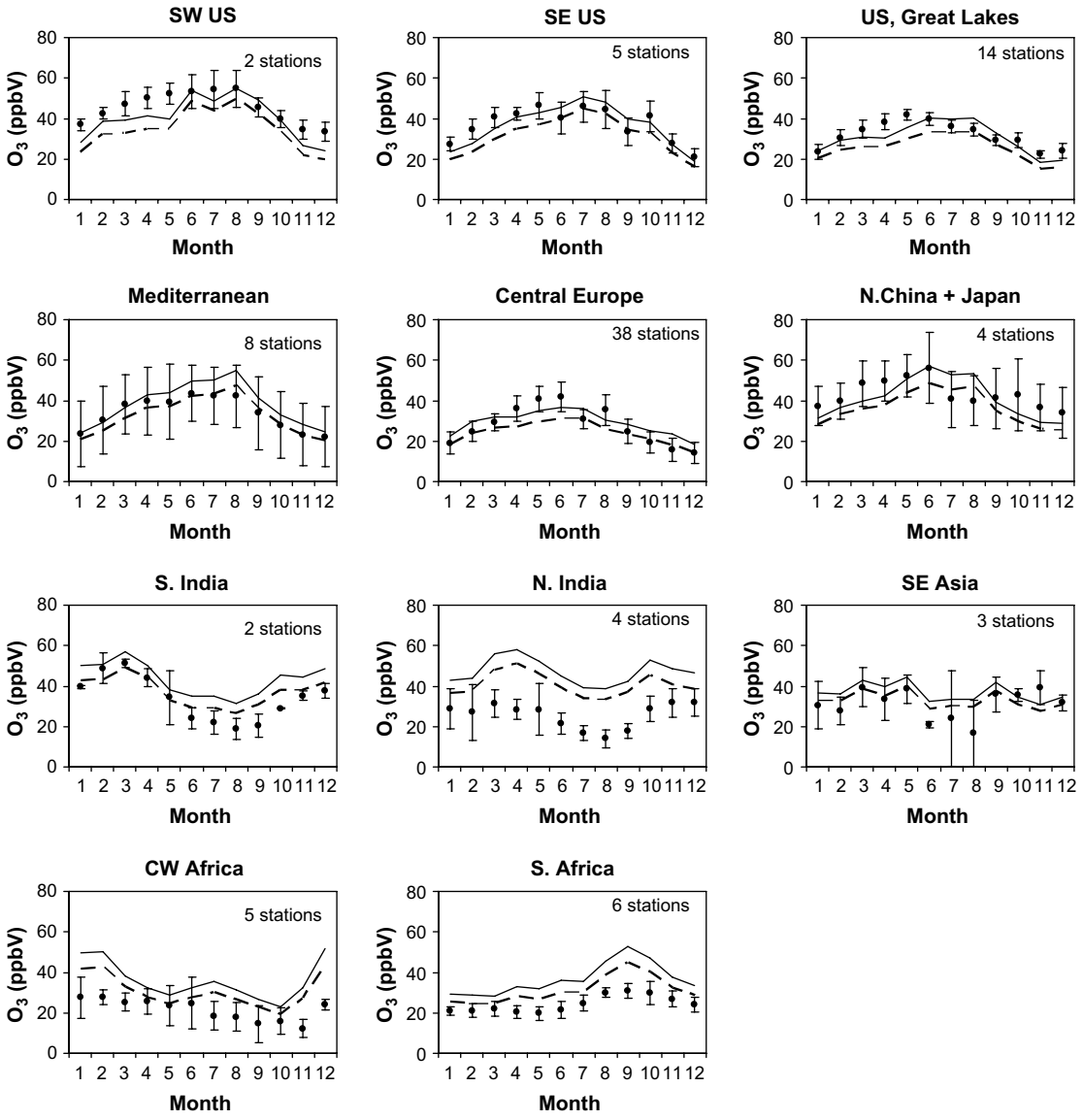

Fig. 6. Comparison between regionally averaged monthly mean ozone concentration from monitoring stations (dots) and TM5 regional model average (lines) for the year 2000. Model results are the means for the model gridboxes where the stations are located. The full line shows the concentration at 30 m altitude, i.e. the center of the surface grid box; the dashed line shows the concentration at 10 m altitude (measurement sampling height). Error bars indicate 1 standard deviation on the available monthly station data.

Table 2
Data sources for intercomparison with the model.

Region	lon, lat (min)	lon, lat (max)	# Of stations	References
South-West USA	−125, 30	−110, 40	2	CASTNET Clean Air Status and Trends Network (http://www.epa.gov/castnet/ozone.html)
South-East USA	−90, 25	−80, 35	5	CASTNET Clean Air Status and Trends Network (http://www.epa.gov/castnet/ozone.html)
USA, Great Lakes	−95, 40	−75, 50	14	CASTNET Clean Air Status and Trends Network (http://www.epa.gov/castnet/ozone.html)
Central Mediterranean	5, 35	30, 45	8	EMEP (http://www.nilu.no/projects/CCC/onlinedata/ozone/index.html), Airbase (http://air-climate.eionet.europa.eu/databases/airbase/airview/index_html)
Central Europe	7, 48	17, 54	38	EMEP (http://www.nilu.no/projects/CCC/onlinedata/ozone/index.html), Airbase (http://air-climate.eionet.europa.eu/databases/airbase/airview/index_html)
Northern China and Japan	110, 35	145, 45	4	World data centre for Greenhouse Gases (http://gaw.kishou.go.jp/wdcgg.html), Akimoto and Pochanart, personal communication, Wang and Mauzerall, 2004, Carmichael et al., 2003
Southern India	75, 10	85, 20	2	Beig et al., 2007, Ahammed et al., 2006
North India + Nepal	70, 20	90, 30	4	Lal et al., 2000, Satsangi et al., 2004, Jain et al., 2005
S.E. Asia	110, 20	125, 35	3	Carmichael et al., 2003
Central-West Africa	−5, 5	15, 15	5	Carmichael et al., 2003, Sauvage et al., 2005
Southern Africa	20, −30	35, −20	6	Zunckel et al., 2004

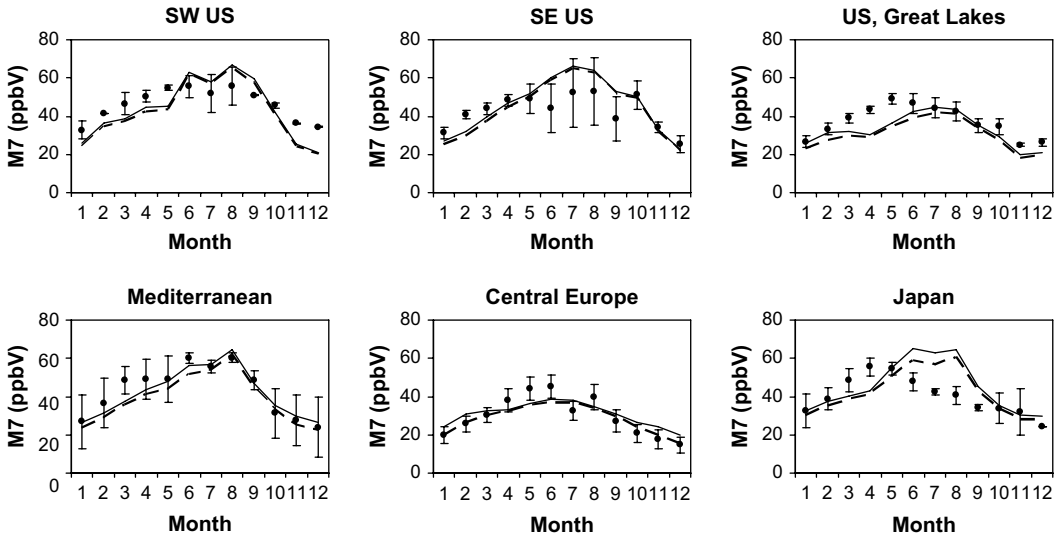

Fig. 7. As in Fig. 6, for monthly averaged M7 (daytime mean ozone from local time 09:00–16:00), for those monitoring stations where hourly ozone data are available. The full line shows the concentration at 30 m altitude, i.e. the center of the surface grid box; the dashed line shows the concentration at 10 m altitude (measurement sampling height). Error bars indicate 1 standard deviation on the available monthly station data.

continent, two distinct ozone episodes are observed: during DJF over equatorial Africa, and during JJA over Angola and the Democratic Republic of Congo, in agreement with observations (Sauvage et al., 2005).

By the year 2030 (Fig. 5a–d), summer time ozone is decreasing by 0–4 ppbV over the Mediterranean area and Central America, thanks to the implementation of air quality legislation. In North-Eastern China, the increased NO_x emissions appear to cause a decrease in ozone levels by 2030, indicating that titration of ozone by NO_x plays a significant role, in particular during the coolest months, and supporting the findings of W&M04. In Western Europe, the opposite effect takes place: decreasing NO_x emissions, with associated decreasing O_3 titration appears to cause an increase of the winter time ozone concentration with about 6–8 ppbV.

As mentioned before, the current version of CLE emissions for India are too pessimistic and lead indeed to a strong increase in O_3 levels with 10 ppbV or more over the Indian continent.

4.2. Comparison of modelled ozone concentration and indicators with measurements

Fig. 6 compares observed and modelled monthly mean surface ozone levels in selected regions for the year 2000. The modelled values are averaged over the grid boxes where the observations are located. The region boundaries, as well as the sources for the measurement data within each region are listed in Table 2. Modelled surface ozone levels are plotted for grid box midpoint (30 m, blue line) as well as at 10 m (yellow line) which is a more realistic value for the sampling height. The observations are averages over data from the several observational sites within each region. Most observations are from ground-based continuous surface UV absorption measurements, except Carmichael et al. (2003) data, which are from passive samplers. We have selected inland measurement sites (except for the Mediterranean area), at an altitude below 650 m. A particular dataset is the one for Central-West Africa, from Sauvage et al. (2005), collected on board

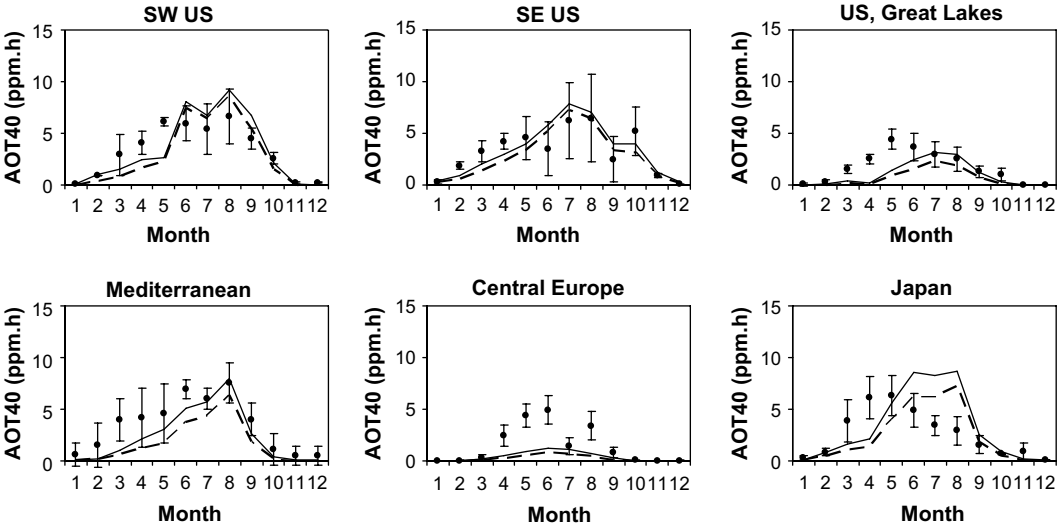

Fig. 8. As in Fig. 6, for monthly accumulated AOT40, for those monitoring stations where hourly ozone data are available. The full line shows the concentration at 30 m altitude, i.e. the center of the surface grid box; the dashed line shows the concentration at 10 m altitude (measurement sampling height). Error bars indicate 1 standard deviation on the available monthly station data.

Table 3
Regionally averaged modelled-to-measured ratio of both metrics during the months May–June–July, at a model height of 30 m and 10 m above the surface respectively.

Region	M7, 30 m	M7, 10 m	AOT40, 30 m	AOT40, 10 m
SW US	1.03	1.01	1.02	0.95
SE US	1.23	1.20	1.25	1.12
US Great Lakes	0.87	0.83	0.60	0.44
Mediterranean	1.07	0.99	0.98	0.73
Central Europe	0.97	0.95	0.37	0.25
Japan	1.33	1.21	1.71	1.27

an in-service Airbus aircraft in the framework of the MOZAIC programme during the flights. From the measured MOZAIC vertical ozone profiles, we used the lowest altitude value available for the locations in Central-West Africa (Lagos, Abidjan, Douala).

The error bars on the measured values represent the standard deviation on the station monthly means. They do not include the individual station's standard deviations on higher temporal scales, nor the analytical uncertainty.

In general, the model is reproducing reasonably well the monthly mean ozone concentrations in regions where quality-controlled ozone monitoring programs are routinely running (Central Europe, U.S.A., Japan). During the summer months, the modelled 10 m concentrations fall within 1 standard deviation of the observations and the seasonal trend is well reproduced. Also for South-East Asia and Southern India we find a satisfactory model performance. In Northern India and the two African regions, the model is significantly overestimating the observed ozone levels. This is particularly of concern for S.-India seen the expected impact on crop losses. The reason for the worse model performance in these regions is not clear a priori. Uncertainties in the emission of ozone precursors may be an important factor, as well as the reduced model resolution over Africa. But also the observational data may not adequately represent the regional-scale ozone concentrations. In fact, out of the 4 N.-Indian measurement stations, 3 are located in densely populated urban areas where ozone levels may be suppressed by local titration, whereas the 4th is a regional station however using a passive sampler as measurement technique.

Indeed, more recent air pollution measurements in the peri-urban and rural areas around Varanasi in the Indo-Gangetic plane (Agrawal et al., 2003) show that summer average ozone concentrations may span from 10 to 58 ppbV, depending on the location relative to the nearby city. In contrast to this, the S.-Indian observations are obtained in peri-urban locations, and in this case the agreement with the model is much better.

We also evaluated the model performance in reproducing monthly accumulated AOT40 and monthly averaged M7 for those locations where hourly ozone data are available (Europe, US and Japan). Results are shown in Fig. 7 (M7) and Fig. 8 (AOT40). Note that for these metrics, obtained during daytime only, the vertical gradient becomes less pronounced than for the monthly means, because of the better vertical mixing of the boundary layer. For M7, the agreement between model and measurements is excellent for south-west and south-east US, the Mediterranean area, and central Europe. For the US Great Lakes region, spring time M7 is underpredicted by 15–20 ppbV but summer months are well reproduced. For Japan, the summer months are significantly over-predicted by up to 20 ppbV. Modelled M7 (as is the case for M12 and the monthly mean) appears not to be very sensitive to the ozone sample height.

The picture looks similar for AOT40 (Fig. 8), but differences between model and measurements are amplified as a consequence of the cumulative nature of the metric in combination with a non-zero threshold (Tuovinen et al., 2007). In particular for Central Europe, the difference between model and measured AOT40 is disturbingly high; other regions are performing better. Table 3

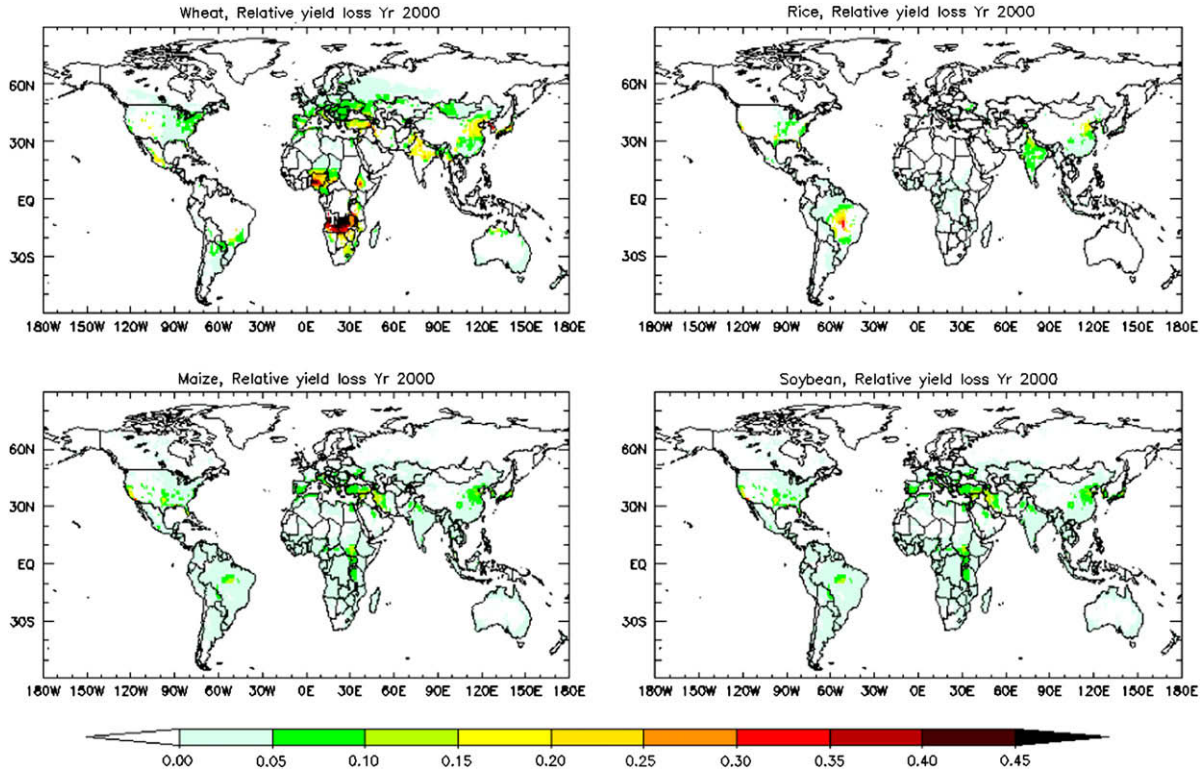

Fig. 9. Average relative yield loss from 2 metrics for the 4 crops, year 2000.

Table 4
Regionally aggregated relative yield loss RYL for wheat, rice, maize and soybean.

	WORLD	EU25	N.Am	China	India
Wheat					
AOT40	12.3%	4.1%	4.1%	19.0%	27.6%
M7	7.3%	4.6%	4.4%	9.8%	13.2%
Rice					
AOT40	3.7%	4.7%	3.2%	3.9%	8.3%
M7	2.8%	3.5%	2.6%	3.1%	5.7%
Maize					
AOT40	2.4%	3.1%	2.2%	4.7%	2.0%
M12	4.1%	5.1%	3.6%	7.1%	4.0%
Soybean					
AOT40	5.4%	20.5%	7.1%	11.4%	4.7%
M12	15.6%	27.3%	17.7%	20.8%	19.1%

shows the regionally averaged modelled-to-measured ratio of AOT40 and M7, accumulated or averaged over the months May–June–July. Table 3 shows the regionally averaged modelled-to-measured ratio of AOT40 and M7, accumulated or averaged over the months May–June–July. On a regional-scale, seasonal M7 is reproduced by the model within 20% (at 10 m above surface). Seasonal modelled AOT40 ranges between 25% and 127% of observed regionally averaged values. This confirms that, from the modelling point of view, AOT40 is a less robust metric for evaluating crop exposure to ozone than concentration averages like M7 (Tuovinen et al., 2007), which obviously introduces considerable uncertainties in the crop loss estimates."

4.3. Crop losses

4.3.1. Year 2000, RYL

Fig. 9 shows global maps of the ozone-induced RYL for each of the 4 crops considered. The RYL shown in the maps is the average of RYL_{AOT} and RYL_{Mi}. Table 4 gives regionally aggregated values for RYL for each of the two indicators. The geographical distribution of the RYL largely reflects the ozone distribution during spring (Central America, US east coast, India, north-east China) and summer (western US, Mediterranean area, southern Africa), and indicates the hotspots with the highest risk. This is particularly clear for the most sensitive crops (wheat and soybean) where locally the RYL exceeds 30%. On a global scale, the RYL for wheat ranges between 7% and 12%, with AOT40 giving the highest value (Table 4). For soybean we obtain a range 5–16% with M12 giving the highest value. Global averaged losses for rice (maize) are in the range 3–4% (3–5%).

Table 4 also lists the regionally aggregated RYL for the European Union (25 countries), North America (U.S. + Canada), China and India. The highest relative losses for wheat are observed in India and China: present day losses for wheat are possibly ranging up to 19% for China and 28% for India. The RYL for rice is significantly higher in India (6–8%) than in the other regions (<5%). For soybean, the highest RYL are found in Europe (20–27%) and China (11–21%). Regionally aggregated maize RYL remains rather limited for all regions (between 2 and 7%).

4.3.2. Year 2000, crop production losses (metric tons) and economic damage (US$)

Fig. 10 shows the geographical distribution of the estimated present-day crop production loss (metric tons/km^2), derived from the gridded average RYL (Fig. 9) and crop production fields (Fig. 3). The plot highlights the vulnerability of high-production areas which are exposed to high ozone concentrations. Some areas with a high RYL in Fig. 9 disappear in this figure because of the low production intensity (e.g. Africa) whereas other areas with a relatively low RYL stand out in Fig. 10 due to the high-production intensity (e.g. maize in the U.S.).

Table 5 gives the regionally aggregated numerical values for the estimated crop production loss. In terms of weight, wheat is by far the most affected crop: globally we estimate a possible loss between 45 and 82 million metric tons, of which 30% occurring in India and 25% in China. Production losses for rice, maize and soybean are of the order 17–23 million metric tons globally. India

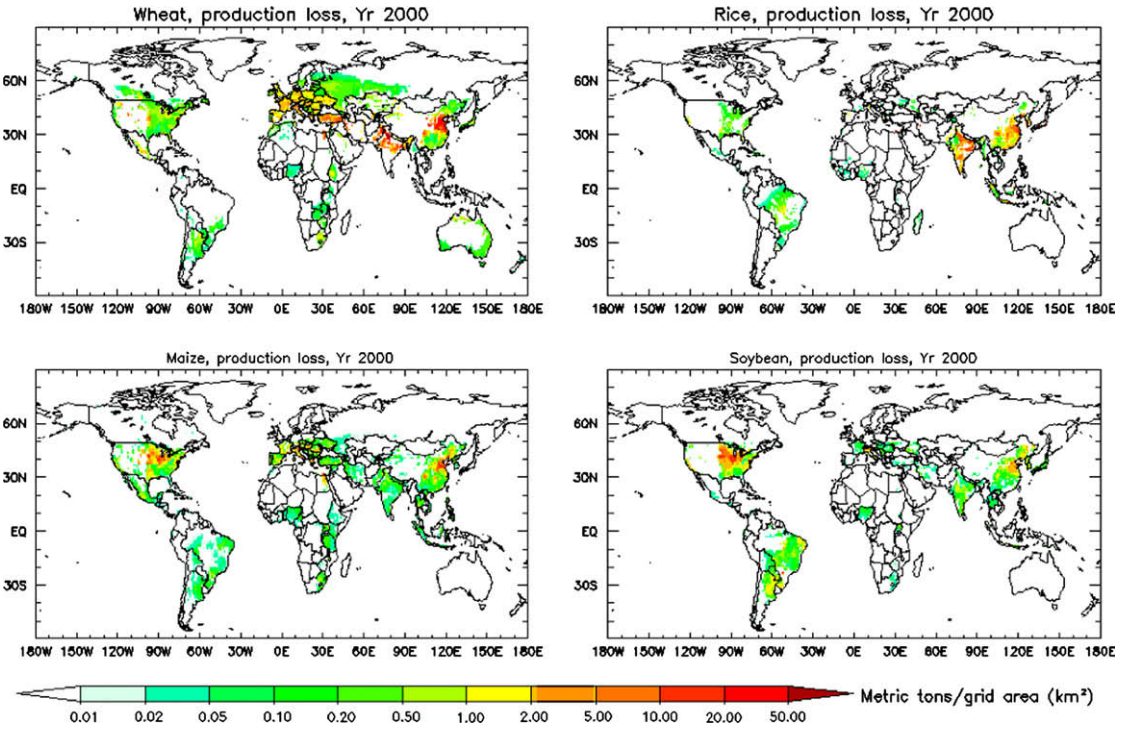

Fig. 10. Average crop production loss from 2 metrics for the 4 crops, year 2000. The production loss numbers are normalized to the grid cell area.

Table 5
Estimated range in crop production loss (year 2000) due to ozone damage, million metric tons, from indicators considered in this study (see text).

	Wheat		Rice		Maize		Soybean	
	Min	Max	Min	Max	Min	Max	Min	Max
World	45.5	81.8	17.1	23.1	14.4	25.2	9.2	29.8
EU25	5.3	6.0	0.09	0.12	1.5	2.5	0.31	0.45
N.Am	3.6	3.9	0.24	0.29	5.8	9.8	5.9	16.7
China	10.8	23.4	6.0	7.7	4.9	7.7	2.0	4.0
India	11.6	29.1	7.7	11.4	0.23	0.5	0.26	1.2

Table 6
Estimated range in economic loss (year 2000) due to ozone damage, million US$, from indicators considered in this study (see text).

	Wheat		Rice		Maize		Soy		Total	
	Min	Max	Min	Max	Min	Max	Min	Max	Min	Max
World	6361	12046	4279	5634	1446	2568	1979	5829	14063	26077
EU25	601	647	23	31	179	294	54	79	857	1051
N.Am.	340	369	29	36	423	717	1005	2845	1798	3967
China	1276	2766	788	1003	505	789	462	946	3030	5504
India	1711	4310	1017	1509	25	51	51	244	2804	6114

and China account for 47% and 37% respectively of the rice production losses. The U.S. is the largest contributor to maize and soybean losses (40%–60% of the global losses respectively). The high losses obtained for India have to be considered with care, seen the large discrepancy between modelled and measured ozone concentrations in Southern India.

Taking into account the producer price, we estimate the present day associated economic damage for the major world regions (Table 6). On a global scale, the crop losses estimated in this study represents an economic value of $14–$26 billion (year 2000). This number is significantly higher than the estimated present-day losses to crops caused by global warming (globally $5 billion per year, Lobell and Field, 2007).

For the European Union, the damage ranges between $0.9 and $1.1 billion, and for N. America (U.S. + Canada) between $1.8 and $4 billion. Results and ranking for individual countries with the most significant losses are shown in Fig. 11. Present day economic losses for China and India are estimated between $3 and $6 billion each. The high ranking of relatively minor producers like Syria, Iran, Japan, S. Korea, Myanmar is due to the fact that producer prices in these countries are a multiple of the global median price (e.g. for Japan the producer prices of each of the crops is a factor 10 times the global median, see FAOSTAT). China and India each account for about 20% of the global economic damage (Table 7). In Table 7 we also compare the estimated economic loss for the crops in this study with the countries' GDP and GDP growth rate for the year 2000. For several developing economies, in particular in Asia, the ozone-induced crop damage offsets a significant part of the GDP growth rate.

In Table 8 we compare the results of this study with previous studies of the "present day" economic cost of ozone damage to crops (US, Europe, Asia). The US studies are based on an econometric model taking into account feedbacks of the changed crop production on demand and market prices, whereas the European and Asian studies applied our approach which is based on a simple multiplication model of yield loss and producer price. Taking into account the number of crops evaluated, and the period of previous studies, we can state that our results are consistent with the earlier studies for the US and Europe. The study of W&M04 evaluated the same crops as in our study. We find a good agreement between our estimates and the W&M study for China and Japan, but for South Korea our results are a factor of 2–3 higher. The major reason for this difference is the higher ozone concentration resulting from our model calculations in this area, leading to a RYL for rice (the dominating crop) of 5–8%, whereas W&M obtain a RYL of 2% for rice in 1990.

4.3.3. Year 2030, trends in RYL

Finally we also present the projected trends in the RYL by the year 2030, based on the CLE scenario. The crop distribution, growing season and suitability indices are kept the same as for the year 2000, hence only the effect of changed emissions on the surface ozone concentration is evaluated. Fig. 12 shows the projected change in the RYL for the major world regions by 2030. The values shown are the average from the 2 indicators considered, while the error bars represent the range. We recall that for India, a worst case scenario of non-action was assumed, explaining the strong increase in crop losses for wheat and soybeans on top of already high-production losses for 2000.

Despite the optimistic scenario, a global increase in the RYL for wheat soybean, maize and rice is expected (+4%, +0.5%, +0.2%,

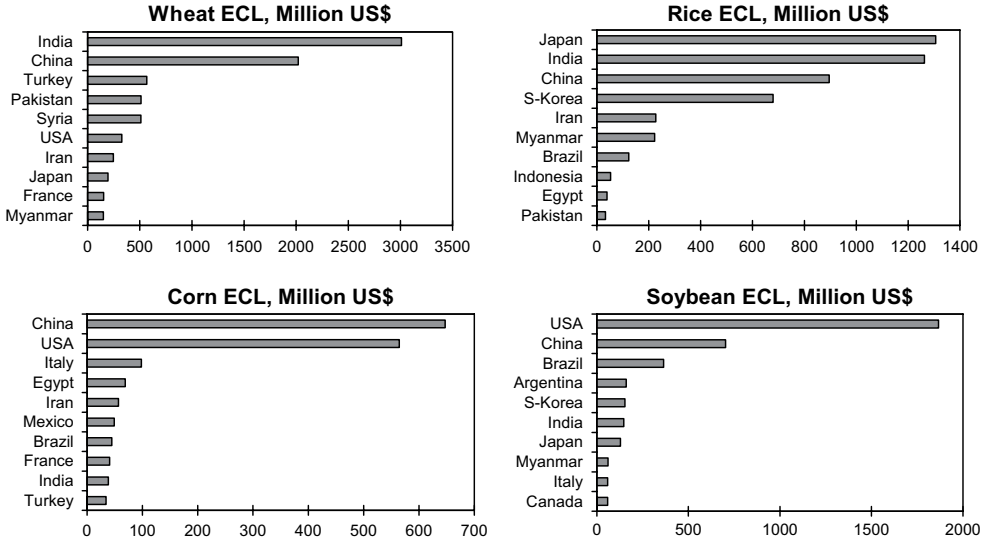

Fig. 11. Estimated economic losses of 10 highest ranked countries for the year 2000.

Table 7
Ranking of countries with highest economic losses (year 2000) at 4 crops considered (average of M and AOT40).

	Econ. Loss (10^6 US$)	Fraction of global loss	GDP 2000[a] (10^6 US$)	4 Crops loss as fraction of GDP	GDP growth rate 2000[a]
India	4459	22%	4.60E + 05	0.97%	4.0%
China	4267	21%	1.20E + 06	0.36%	8.4%
USA	2791	14%	9.76E + 06	0.03%	3.7%
Japan	1631	8%	4.65E + 06	0.04%	2.9%
S.-Korea	839	4%	5.12E + 05	0.16%	8.5%
Turkey	617	3%	1.99E + 05	0.31%	7.4%
Iran	584	3%	1.01E + 05	0.58%	5.1%
Pakistan	557	3%	7.33E + 04	0.76%	4.3%
Brazil	545	3%	6.44E + 05	0.08%	4.3%
Syria	532	3%	1.93E + 04	2.8%	2.7%

[a] Source: World Development Indicators database, World Bank; http://go.worldbank.org/4C55Z0H7Z0.

+1.7% respectively). Excluding India from the global average does not affect these numbers significantly. Europe, Northern America and China (except for rice) show a stabilisation or improvement of the year 2000 situation.

Table 9 shows the projected trend in RYL for individual countries with most significant changes in RYL by 2030. The upper part of the table lists the countries with the worst results in relative yield compared to the base case. As expected, South-East Asia is mostly affected. The countries with strongest improvements are listed in the lower part of Table 9. Most countries listed are located in the Central and East Mediterranean area, as expected from the projected decrease in summer time ozone levels under the CLE scenario (Fig. 5f). Also Mexico is expected to slightly improve the situation for wheat, rice and soybean.

5. Discussion of caveats and uncertainties

Although this study is the first to evaluate ozone damage to crops on a global scale, we recognize that several uncertainties and caveats have to be considered. An integrated assessment inevitably accumulates the uncertainties embedded in each of its components. It was not within the scope of this study to conduct a detailed and quantitative error propagation analysis. As a first evaluation of the uncertainty range on our results we refer to Holland et al. (2006) who calculated for the European region the contribution of various factors onto the uncertainty on AOT40 and the associated economic loss. Taking into account the variability between years in crop production, the variability between years in ozone concentration, the variation of the vertical ozone profile near the crop canopy, the uncertainty in the growing season, the uncertainty on the exposure-response function, the variation in crop price, they obtain as an overall uncertainty range on the economic losses 33% to +40% (90% confidence interval).

The latter study is however limited to Europe, and more importantly it does not consider the model performance in terms of AOT40. In our study we find, based on model-measurement intercomparison, that AOT40 is well represented in N.-America, but may be under-predicted by up to 70% in Central Europe. Unfortunately a proper evaluation of the model performance in terms of AOT40 in most of Asia or Africa is not possible due to lack of ozone measurements at hourly time resolution.

On top of the model performance, a second major additional uncertainty in our study lies in the application of pooled E–R relationships, derived for European and North-American crops, to crops over the globe without taking into account possible biases in ozone sensitivity for particularly Asian cultivars. Due to a lack of data, the introduced uncertainty is difficult to quantify, but as mentioned before, a few small scale studies indicate that Asian crops are at least as sensitive to ozone damage as western crops.

In Table 10 we give a qualitative evaluation of the confidence we give to different components of the integrated assessment for each of the major regions considered in this study. The results for N.-America have the highest confidence thanks to the good performance on all criteria. European results are likely to be underestimated, in particular in Central Europe when based on AOT40. For China the model performance is satisfactory (at least for the monthly 24 h means), but the lack of information on crop sensitivity probably leads to an underestimation of the crop losses. The apparent over-prediction of monthly mean ozone in N.-India and Africa may be partly offset by the underestimation of crop sensitivities (Emberson et al., submitted for publication), but the final magnitude and impact on the results cannot be evaluated.

Regarding the projections for the year 2030, we recall that the underlying emission scenario is relatively optimistic, as the implementation of legislation usually does not happen at 100% efficiency. Our estimates for changes by 2030 therefore have to

Table 8
Overview of studies on the economic damage resulting from ozone damage to crops, together with results from this study.

Country	Commodities	Year	Economic damage (million US$)		References	Indices used	Econ. model
			Min	Max			
US	Maize, wheat, rice, soybeans, cotton, alfalfa, sorghum, forage	1982	1890		Adams et al., 1987	M7/M12	[a]
US	Maize, wheat, rice, soybeans, cotton, alfalfa, sorghum, barley	1990	2000	3300	Murphy et al., 1999	M7/M12	[a]
US	Maize, wheat, rice, soybeans	2000	1741	3840	This study	M7/M12, AOT40	[b]
EU25	23 crops	2000	4255		Holland et al., 2006	AOT40	[b]
EU25	Maize, wheat, rice, soybeans	2000	857	1051	This study	M7/M12, AOT40	[b]
China	Maize, wheat, rice, soybeans	1990	3468	4128	Wang and Mauzerall, 2004	M7/M12, SUM06, W126	[b]
China	Maize, wheat, rice, soybeans	2000	3030	5504	This study	M7/M12, AOT40	[b]
Japan	Maize, wheat, rice, soybeans	1990	1105	1167	Wang and Mauzerall, 2004	M7/M12, SUM06, W126	[b]
Japan	Maize, wheat, rice, soybeans	2000	1220	2040	This study	M7/M12, AOT40	[b]
Korea	Maize, wheat, rice, soybeans	1990	239	308	Wang and Mauzerall, 2004	M7/M12, SUM06, W126	[b]
Korea	Maize, wheat, rice, soybeans	2000	639	1039	This study	M7/M12, AOT40	[b]

[a] Econometric model based on microeconomic model taking into account feedbacks of changes in production due to air pollution on market prices and demand.
[b] Simple multiplication of yield loss with commodity market (producer) price.

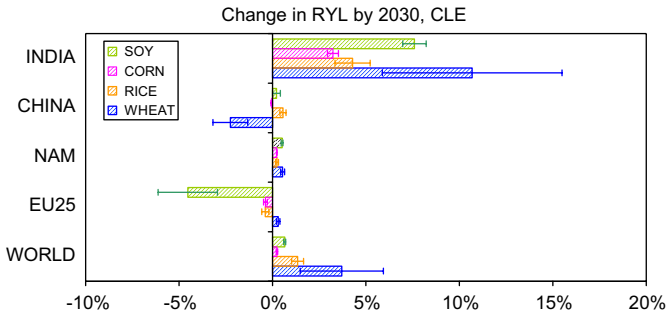

Fig. 12. Projected change in the relative yield loss by 2030 under implementation of current legislation for the globe and major world regions (India: no legislation assumed). Negative numbers indicate a lower loss. Bars: average of AOT40 and M7/M12 based loss estimate. Error bars indicate the range between lowest and highest values.

Table 9
Countries with highest (positive or negative) projected changes in relative crop yield from 2000 to 2030, based on averaged RYL from M7/M12 and AOT40.

Wheat		Rice		Maize		Soybean	
Highest increase in relative yield loss S2–S1							
+26.3%	Pakistan	+6.4%	Pakistan	+10.7%	Pakistan	+28.1%	Pakistan
+16.7%	Bangladesh	+4.3%	India	+3.7%	Bangladesh	+7.6%	India
+10.7%	India	+1.3%	Tajikistan	+3.2%	India	+5.8%	Nepal
+6.9%	Nepal	+1.0%	N.-Korea	+3.0%	N.-Korea	+3.9%	Morocco
+6.0%	N.-Korea			+1.9%	Lesotho	+3.7%	Philippines
+5.3%	Nigeria			+1.8%	S.-Korea	+3.5%	S.-Korea
+4.5%	Lesotho					+3.2%	Nigeria
+3.6%	South Africa					+3.2%	Tajikistan
+2.8%	Tajikistan					+3.1%	South Africa
+2.7%	Rwanda					+2.9%	Indonesia
Highest decrease in relative yield loss S2–S1							
−3.3%	Turkey	−2.0%	Turkey	−1.7%	Turkey	−5.5%	Italy
−2.3%	China	−1.1%	Portugal	−1.6%	Syria	−3.8%	Turkey
−1.9%	Slovenia	−1.1%	Italy	−1.4%	Italy	−3.5%	Syria
−1.7%	Mexico	−0.4%	Mexico	−1.2%	Lebanon	−1.9%	Slovenia
−1.4%	Italy	−0.3%	Greece	−0.6%	Slovenia	−1.2%	Mexico
−1.3%	Syria	−0.3%	Hungary	−0.4%	Greece	−1.1%	Greece
−1.3%	Lebanon					−0.9%	Spain

be considered as conservative, except for India where we may expect an improved situation compared to the results shown here.

An additional source of uncertainty for the year 2030 RYL projections which is difficult to quantify is the not-accounted role of feedback mechanisms between climate change and ozone levels, as well as the effect of changing CO_2 levels on stomatal deposition. The feedbacks to consider are

- change in meteorology, affecting ambient ozone levels even with constant emissions (Langner et al., 2005)
- change in meteorology (temperature, humidity, soil water, …) affecting the growing season, crop distribution, and stomatal dose itself
- increase in CO_2, reducing stomatal conductance, hence reducing stomatal ozone uptake, but simultaneously increasing ambient ozone levels (Harmens et al., 2007)
- change in biogenic emissions of ozone precursors due to changing climate

For the year 2030, these effects will be rather limited, but a truly integrated long term assessment of the impact of both climate change and air quality onto future crop yield and production can only be based on a stomatal uptake approach, not only for crops and forests but for any type of vegetation, linked to an economic model which takes into account changing conditions of supply and demand to drive changing crop production patterns.

6. Conclusion

Using a global chemistry transport model, we have estimated the risk to crop damage caused by surface ozone based on two types of exposure indicators (seasonally mean daytime ozone concentration, and seasonally accumulated daytime ozone concentration above 40 ppb). Two model runs were analyzed, based on present day emissions (year 2000) and based on a fairly optimistic "Current Legislation" scenario, assuming that all legislation in place today will be fully implemented by 2030.

Although AOT40 is the operational metric for evaluating crop exposure to ozone in European legislation, its low robustness (sensitivity to changes and uncertainties in input values) makes it less suitable as a modelled indicator for crop losses. M7 is performing satisfactorily from modelling point of view, but it is considered as a less suitable indicator for crop exposure.

Present day global relative yield losses for wheat are estimated to range between 7% and 12% for wheat, between 6% and 16% for soybean, between 3% and 4% for rice, and between 3% and 5% for maize (ranges resulting from different metrics used). The unquantified uncertainty caused by model performance and crop sensitivity is not included in this range. Taking into account probable biases introduced through the global application of "western" crop exposure–response functions, and model performance in reproducing ozone-exposure metrics, our estimates may be considered as being conservative.

In terms of absolute production losses, wheat and rice are most affected. Translating the production losses into total global economic damage for the four crops considered, using world market prices for the year 2000, we estimate a global economic loss in the range $14–$26 billion. About 40% of this damage is occurring in China and India. Considering the recent upward trends in crop and food prices, the ozone-induced damage to crops is expected to offset a significant portion of the GDP growth rate, especially in countries with an economy based on agricultural production.

Implementation of current air quality legislation will lead by 2030 to a reduction of losses mostly in developed countries, together with China where a slight improvement is expected. In the rest of Asia and in parts of Africa, current legislation is not sufficient to stabilize or improve air quality by 2030.

Table 10
Qualititative evaluation of the level of confidence given to the regionally aggregated crop losses. The +/−/0 signs indicate if the uncertainty leads to over/under prediction or no bias (0).

	Model performance		Exposure–response functions	Overall confidence
	M7/M12	AOT40		
North-America	High (0)	Medium-high (0)	High (0)	High (0)
EU25	High (0)	Low-medium (−)	High (0)	Medium (−)
China	Medium (0)	Medium (?)	Medium (−?)	Medium (−?)
India	Low-medium (+)	Low (+?)	Low (−?)	Low
Africa	Low	Low	Low	Low

Acknowledgments

The authors gratefully acknowledge support from the EU-funded ACCENT 'Network of Excellence' (contract no. 505337), and from the EU Integrated Project EUCAARI (contract no. 036833). We gratefully thank P. Ponachart and H. Akimoto for sharing unpublished data from the MEXT project (Research Revolution 2002) and A. Fiore for processing CASTNET ozone data. The comments and suggestions of one anonymous reviewer have substantially improved the quality of the paper.

Appendix. Supplementary material

Supplementary material associated with this article can be found in the online version, at doi:10.1016/j.atmosenv.2008.10.033.

References

Adams, R.M., Crocker, T.D., Thanvaibulchai, N., 1982. An economic assessment of air pollution damages to selected annual crops in southern California. Journal of Environmental Economics and Management 9, 42–58.

Adams, R.M., Glyer, D.J., McCarl, B.A., 1987. The NCLAN economic assessment: approach, findings and implications. In: Heck, W.W., Taylor, O.C., Tingey, D.T. (Eds.), Assessment of Crop Losses from Air Pollutants. Elsevier Applied Sience, London.

Agrawal, M., Singh, B., Rajput, M., Marshall, F., Bell, J.N.B., 2003. Effect of air pollution on peri-urban agriculture: a case study. Environmental Pollution 126, 323–329.

Ahammed, Y.N., Reddy, R.R., Gopal, K.R., Narasimhulu, K., Basha, D.B., Reddy, L.S.S., Rao, T.V.R., 2006. Seasonal variation of the surface ozone and its precursor gases during 2001–2003, measured at Anantapur (14.62°N), a semi-arid site in India. Atmospheric Research 80, 151–164.

Aunan, K., Berntsen, T.K., Seip, H.M., 2000. Surface ozone in China and its possible impact on agricultural crop yields. Ambio 29, 294–301.

van Aardenne, J.A., Carmichael, G.R., Levy II, H., Streets, D., Hordijk, L., 1999. Anthropogenic NO(x) emissions in Asia in the period 1990–2020. Atmospheric Environment 33, 633–646.

Beig, G., Gunthe, S., Jadhav, D.B., 2007. Simultaneous measurements of ozone and its precursors on a diurnal scale at a semi urban site in India. Journal of Atmospheric Chemistry 57, 239–253.

Carmichael, G.R., et al., 2003. Measurements of sulfur dioxide, ozone and ammonia concentrations in Asia, Africa, and South America using passive samplers. Atmospheric Environment 37, 1293–1308.

Dentener, F., Stevenson, D., Cofala, J., Mechler, R., Amann, M., Bergamaschi, P., Raes, F., Derwent, R., 2005. The impact of air pollutant and methane emission controls on tropospheric ozone and radiative forcing: CTM calculations for the period 1990–2030. Atmospheric Chemistry and Physics 5, 1731–1755.

Dentener, F., et al., 2006. The global atmospheric environment for the next generation. Environmental Science and Technology 40, 3586–3594.

Emberson, L.D., Büker, P., Ashmore, M.R., Mills, G., Jackson, L., Agrawal, M., Atikuzzaman, M.D., Cinderby, S., Engardt, M., Jamir, C., Kobayashi, K., Oanh, K., Quadir, Q.F., Wahid, A. Dose–response relationships derived in North America underestimate the effects of ozone (O_3) on crop yields in Asia. Atmospheric Environment, submitted for publication.

Fischer, G., van Velthuizen, H., Nachtergaele, F., Medow, S., 2000. Global Agro-Ecological Zones (Global – AEZ) [CD-ROM and web site. Available from: http://www.fao.org/ag/AGL/agll/gaez/index.htm], Food and Agricultural Organization/International Institute for Applied Systems Analysis (FAO/IIASA). Available from: http://www.iiasa.ac.at/Research/LUC/GAEZ/index.htm.

Fuhrer, J., Skärby, L., Ashmore, M.R., 1997. Critical levels for ozone effects on vegetation in Europe. Environmental Pollution 97, 91–106.

Harmens, H., Mills, G., Emberson, L.D., Ashmore, M.R., 2007. Implications of climate change for the stomatal flux of ozone: a case study for winter wheat. Environmental Pollution 146, 763–770.

Heck, W.W., Taylor, O.C., Tingey, D.T. (Eds.), 1987. The NCLAN economic assessment: approach, findings and implications. In: Assessment of Crop Losses from Air Pollutants. Elsevier Applied Sience, London.

Holland., M., Mills, G., Hayes, F., Buse, A., Emberson, L., Cambridge, H., Cinderby, S., Terry, A., Ashmore, M., 2002. Economic assessment of crop yield losses from ozone exposure. Report to U.K. Department of Environment, Food and Rural affairs under contract 1/2/170, Centre for Ecology and Hydrology, Bangor.

Holland, M., Kinghorn, S., Emberson, L., Cinderby, S., Ashmoe, M., Mills, G., Harmens, H., 2006. Development of a framework for probabilistic assessment of the economic losses caused by ozone damage to crops in Europe. CEH Project No. C02309NEW. Report to U.K. Department of Environment, Food and Rural affairs under contract 1/2/170 1/3/205.

Jain, S.L., Arya, B.C., Kumar, A., Ghude, S.D., Kulkarni, P.S., 2005. Observational study of surface ozone at New Delhi, India. International Journal of Remote Sensing 26, 3515–3524.

Krol, M., Houweling, S., Bregman, B., vandenBroek, M., Segers, A., van Velthoven, P., Peters, W., Dentener, F., Bergamaschi, P., 2005. The two-way nested global chemistry-transport zoom model TM5: algorithm and applications. Atmospheric Chemistry and Physics 5, 417–432.

Krupa, S.V., Nosal, M., Legge, A.H., 1998. A numerical analysis of the combined open-top chamber data from the USA and Europe on ambient ozone and negative crop responses. Environmental Pollution 101, 157–160.

Lal, S., Naja, M., Subbaraya, B.H., 2000. Seasonal variations in surface ozone and its precursors over an urban site in India. Atmospheric Environment 34, 2713–2724.

Langner, J., Bergström, R., Foltescu, V., 2005. Impact of climate change on surface ozone and deposition of sulphur and nitrogen in Europe. Atmospheric Environment 39, 1129–1141.

Legge, A.H., Grunhage, L., Noal, M., Jager, H.J., Krupa, S.V., 1995. Ambient ozone and adverse crop response: an evaluation of north American and European data as they relate to exposure indices and critical levels. Journal of Applied Botany 69, 192–205.

Li, X., He, Z., Fang, X., Zhou, X., 1999. Distribution of surface ozone concentration in the clean areas of China and its possible impact on crop yields. Advances in Atmospheric Sciences 16, 154–158.

Lin, C.-Y., Jacob, D.D., Fiore, A.M., 2001. Trends in exceedances of the ozone air quality standard in the continental United States. Atmospheric Environment 35, 3217–3228.

Lobell, D.B., Field, C.B., 2007. Global scale climate-crop yield relationships and the impact of recent warming. Environmental Research Letters 2. doi:10.1088/1748-9326/2/1/014002.

LRTAP Convention, 2004. Manual on Methodologies and Criteria for Modelling and Mapping Critical Loads and Levels and Air Pollution Effects, Risks and Trends. International Cooperative Programme on Mapping and Modelling under the UNECE Convention on Long-Range Transboundary Air Pollution. Available from: http://www.oekodata.com/icpmapping/.

Mauzerall, D.L., Wang, X., 2001. Protecting agricultural crops from the effects of tropospheric ozone exposure: Reconciling science and standard setting in the United States, Europe, and Asia. Annual Review of Energy and the Environment 26, 237–268.

Mills, G., Buse, A., Gimeno, B., Bermejo, V., Holland, M., Emberson, L., Pleijel, H., 2007. A synthesis of AOT40-based response functions and critical levels of ozone for agricultural and horticultural crops. Atmospheric Environment 41, 2630–2643.

Murphy, J.J., Delucchi, M.A., McCubbin, D.R., Kim, H.J., 1999. The cost of crop damage caused by ozone air pollution from motor vehicles. Journal of Environmental Management 55, 273–289.

Olivier, J.G.J., Berdowski, J.J.M., 2001. Global emissions sources and sinks. In: Berdowski, J., Guicherit, R., Heij, B.J. (Eds.), The Climate System. A.A. Balkema Publishers/Swets & Zeitlinger Publishers, Lisse, The Netherlands, pp. 33–78.

Satsangi, G.S., Lakhani, A., Kulshrestha, P.R., Taneja, A., 2004. Seasonal and diurnal variation of surface ozone and a preliminary analysis of exceedance of its critical levels at a semi-arid site in India. Journal of Atmospheric Chemistry 47, 271–286.

Sauvage, B., Thouret, V., Cammas, J., Gheusi, F., Athier, G., Nédélec, P., 2005. Tropospheric ozone over Equatorial Africa: Regional aspects from the MOZAIC data. Atmospheric Chemistry and Physics 5, 311–335.

Solberg, S., Lindskog, A. (Eds.), 2005. The Development of European Surface Ozone. Implications for a Revised Abatement Policy EMEP/CCC-Report 1/2005. Available from: http://www.nilu.no/projects/CCC/reports/cccr1-2005.pdf.

Stevenson, D.S., et al., 2006. Multimodel ensemble simulations of present-day and near-future tropospheric ozone. Journal of Geophysical Research D: Atmospheres 111. doi:10.1029/2005JD006338.

Tuovinen, J., Simpson, D., Emberson, L., Ashmore, M., Gerosa, G., 2007. Robustness of modelled ozone exposures and doses. Environmental Pollution 146, 578–586.

USDA, United States Department of Agriculture, 1994. Major World Crop Areas and Climatic Profiles. In: Agricultural Handbook No. 664. World Agricultural Outlook Board, U.S. Department of Agriculture. Available from: http://www.usda.gov/oce/weather/pubs/Other/MWCACP/MajorWorldCropAreas.pdf.

Wang, X., Mauzerall, D.L., 2004. Characterizing distributions of surface ozone and its impact on grain production in China, Japan and South Korea: 1990 and 2020. Atmospheric Environment 38, 4383–4402.

Zunckel, M., Venjonoka, K., Pienaar, J.J., Brunke, E.-G., Pretorius, O., Koosialee, A., Raghunandan, A., VanTienhoven, A.M., 2004. Surface ozone over southern Africa: synthesis of monitoring results during the Cross border Air Pollution Impact Assessment project. Atmospheric Environment 38, 6139–6147.